Crossover behavior in static and dynamic properties of a single DNA molecule from three to quasi-two dimensions

Hitoshi Uemura,* Masatoshi Ichikawa,† and Yasuyuki Kimura‡
Department of Physics, School of Sciences, Kyushu University, 6-10-1 Hakozaki, Higashi-ku, Fukuoka 812-8581, Japan
(Received 19 January 2010; published 4 May 2010)

We studied the conformation and dynamics of a single DNA molecule in a thin slit by a fluorescent microscope. In a slit thinner than the Flory radius in three dimensions, the length of the major axis, the translational self-diffusion coefficient and the rotational relaxation time in a dilute solution show the apparent dependence on the thickness of the slit. The observed dependence is in agreement with that predicted by blob theory, despite the number of blobs is very small. The radial distribution of the segments around the center of mass of a single molecule was also studied and compared with that calculated for a Gaussian and an excluded volume chain. The influence of the polymer concentration on the geometrical confinement by slits was also studied in a semidilute solution near the overlap concentration c^*. The confinement effect is found to be not so serious near c^* and is only significant in the so-called "two-dimensional pancake" region.

DOI: 10.1103/PhysRevE.81.051801 PACS number(s): 61.25.he, 82.35.Pq, 87.15.B−, 87.15.H−

I. INTRODUCTION

Macroscopic physical properties of polymers are unique, and polymers are considered as typical examples of soft condensed matters [1–3]. They have been intensively studied using various kinds of experimental techniques. Among them, the scattering methods with x ray, neutron beam and visible or infrared light are one of the powerful methods to study their static and the dynamic properties [1,3,4]. By combining those scattering methods, one can obtain valuable information on the averaged physical properties from nano- to micrometer scale.

On the contrary to those methods in "reciprocal (wave number) space," the direct observation of a single polymer in "real space" also offers the variable information on its physical properties [5–7]. In addition, fluorescently labeled DNA molecules with long chain length are often utilized for the study of dynamical properties [8,9]. One can directly observe the conformation and dynamics of a single DNA molecule using a fluorescent microscope [8–18]. For example, the overall shape of a molecule and its temporal fluctuation can be studied not only in equilibrium [11,12] but also in nonequilibrium or under external fields [13–18]. These observations also give a chance to confirm the basic theoretical predictions on the physical properties of polymers and the results of computer simulation. To utilize DNA has another advantage that ones extract from a single species are naturally monodisperse. The wide distribution of chain length often makes it difficult to compare the experimental results with theories.

The dependence of the size and the physical properties of polymers on the degree of polymerization (or molecular weight) is the characteristic feature in polymer systems. The scaling concept introduced by de Gennes [1] is powerful theoretical approach to such complex systems. One of the unique applications of the scaling theory is a polymer solution in a confined system, such as a thin slit, a narrow tube or a small pore [1,3,19,20]. The dependence of the size and the physical properties on the degree of confinement is given by a simple power law of the spatial size of the containers. Recently, these scaling predictions in confined systems have been directly tested in a thin slit or a narrow tube which is realized by the nanodesigned architectures [21–26]. The obtained information on the physical properties in such systems is important for designing microfluidic devices utilizing for the transport of polymers and for applying them to the separation of polymers by their sizes.

In this paper, we studied the lateral size, the self-diffusion coefficient and the rotational relaxation time of a single DNA molecule in a slit whose thickness is in the crossover region from three to quasi-two dimensions. After the short description of our experimental method and the theoretical predictions by blob picture, the experimental results for a dilute solution and for a semidilute solution near the overlap concentration are discussed. One can usually obtain the density correlation function (or the radial distribution of the segments) for the ensemble of polymers by scattering methods. However, that for a single polymer has not been obtained by the scattering methods. In this study, we also report the radial distribution of the segments around the center of mass and the length fluctuation of a single polymer in a dilute solution.

II. EXPERIMENT

A. Preparation of DNA sample

The DNA used in this study is T4GT7 DNA (Nippon Gene) whose size is about 166kbp or 56 μm in contour length. The DNA was resolved in a TE buffer solution (5 mM Tris-HCl, 0.5 mM EDTA) containing 4% (v/v) 2-mercaptoethanol, 4.6 mg/ml glucose, 0.2 mg/ml glucose oxidase, and 0.036 mg/ml catalase. Major groove binding fluorescent dye, YOYO-1, was added as a probe of a single

*Present address: Optics and Electronics Laboratory, Fujikura Ltd., Sakura, Chiba 285-8550, Japan.
†Present address: Department of Physics, Kyoto University, Kyoto 606-8502, Japan; ichi@scphys.kyoto-u.ac.jp
‡kimura@phys.kyushu-u.ac.jp

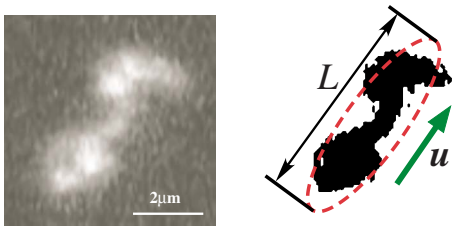

FIG. 1. (Color online) Fluorescent image of a single DNA molecule (left) and its binarized image (right). The ellipsoid drawn as a dotted line is the best-fitted one to the binarized image. **u** is the unit vector parallel to the major axis. L is the length of the major axis.

DNA molecule. The ratio of the dye to a base pair (bp) was 1:7. The concentration of a DNA solution studied was 0.5 μM (bp) for a dilute solution and 33 μM (bp) for a semidilute solution near the overlap concentration [21.1 μM (bp)]. In the case of a semidilute solution, the small amount of fluorescently labeled DNA was mixed with large amount of nonlabeled DNA (1:66 in the molar ratio) to minimize the background illumination from other molecules [12].

The shortage of utilizing fluorescent labeled DNA is that the intercalating dye tends to elongate DNA chains. According to the detail study of this effect, dyes extend the contour length as large as 20–30 % of its original length depending on the concentration of dyes [9]. In our case, this effect makes the size of a molecule a little bit larger. The other shortcoming is that the photobleaching of dyes limits the time of observation, and the irradiation of the excitation light sometimes breaks the DNA during the observation. To reduce the latter effect in data analysis, only the long chains without breaking during observation are used at data analysis.

A DNA solution was sandwiched between two cover glasses (Matsunami Glass Ltd.), and their separation was controlled between 1 and 20 μm by the volume of the solution. The solution was spread to cover the surfaces of glasses fully. To increase the affinity of glass surface to water, the cover glasses were left at 500 °C to make them more hydrophilic before used. The inhomogeneity of the thickness was checked by the interference pattern. The sides of the cell were enclosed by hydrophobic liquid blocker (Funakoshi) to avoid the overflow, the evaporation and the convection of the solution.

B. Measurement method and data analysis

Fluorescent images were obtained by a fluorescent microscope (TE2000, Nikon) with ×100 oil-immersion objective lens (Ph Plan Fluor & Plan Apo, Nikon). The images of a single DNA molecule are captured by a CCD camera (ADT-33B, Flovel) with the sampling rate of 30 frames/s. The sequential images were recorded on a personal computer as movie data.

Figure 1 shows a typical snapshot of a DNA molecule. It exhibits fluctuation of its shape and translationally diffuses inside a glass cell. First, the fluorescent images are converted to the binarized images with appropriate threshold brightness (the image at the right-hand side in Fig. 1). The obtained

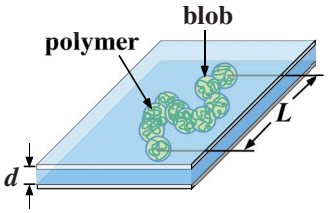

FIG. 2. (Color online) Blob picture of a polymer confined in a slit. A sphere (online yellow) represents a blob with the size d. d is the thickness of the slit, and L is the lateral size of the polymer.

binarized image is fitted to an ellipsoid with the same position of the center of mass, the same area and the same second moment. We regard the center of mass of the binarized image as that of the DNA molecule and the length of its major axis L as its size.

Mean square displacement (MSD) was calculated from the two-dimensional position of the center-of-mass $\boldsymbol{R}_m(t)$ from sequential images as

$$\mathrm{MSD} = \langle [\boldsymbol{R}_m(t+\Delta t) - \boldsymbol{R}_m(t)]^2 \rangle = 4D\Delta t, \tag{1}$$

where D is the translational self-diffusion coefficient, and Δt is the lag time.

The rotational relaxation time τ of a DNA molecule was estimated from the time correlation function of the unit vector $\boldsymbol{u}(t)$ parallel to the major axis as shown in Fig. 1. The calculated correlation function was fitted to an exponentially decaying one with a single relaxation time τ as

$$\langle \mathbf{u}(t+\Delta t) \cdot \mathbf{u}(t) \rangle = \exp(-\Delta t/\tau). \tag{2}$$

III. BLOB THEORY OF A POLYMER IN A THIN SLIT

When a polymer is placed in a thin slit whose thickness d is smaller than the size of a polymer in three-dimensional free space, it can be modeled as a train of spherical units called "blobs" whose sizes are identical to d as schematically shown in Fig. 2 [1,3,19,20]. The confined polymer is an excluded volume chain composed of blobs in two dimensions. Inside a blob, a polymer chain behaves as an excluded volume chain in three dimensions. Therefore, the following relationships are expected to be held:

$$d = bn^{\nu(3)}, \tag{3}$$

$$N = mn, \tag{4}$$

$$L = dm^{\nu(2)}. \tag{5}$$

In Eqs. (3)–(5), N is the number of segments in a polymer, b is the Kuhn length, m is the number of the blobs in the polymer, n is the number of the segments inside a blob, d is the thickness of the slit, and L is the lateral size of the polymer. The exponent $\nu(2)$ and $\nu(3)$ are, respectively, the Flory exponents in two and three dimensions [1–3]. From Eqs. (3)–(5), L is given as

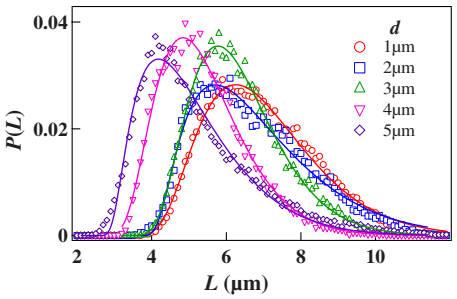

FIG. 3. (Color online) Distribution of the length of the major axis L, $P(L)$, in a slit with different thickness d. The solid lines are the best-fitted ones with Eq. (12). The best-fitted values of $L_{\min}$ are respectively 2.33, 2.97, 2.41, 1.82, and 2.28 μm for $d=1$, 2, 3, 4, and 5 μm.

$$L = N^{\nu(2)} b^{\nu(2)/\nu(3)} d^{1-\nu(2)/\nu(3)}. \tag{6}$$

In a good solvent, $\nu(2)$ and $\nu(3)$ are, respectively, $\nu(2)=3/4$ and $\nu(3)=3/5$ [1–3]. The dependence of L on d is given as

$$L = bN^{3/4}\left(\frac{b}{d}\right)^{1/4} \propto d^{-1/4}. \tag{7}$$

When the hydrodynamic interaction between blobs is ignored, the translational self-diffusion coefficient D can be scaled as

$$D \propto \frac{1}{md}. \tag{8}$$

From Eqs. (3) and (4), the dependence of D on d is given as

$$D \propto d^{1/\nu(3)-1} = d^{2/3}. \tag{9}$$

The rotational relaxation time τ is estimated as the time in which a polymer translationally diffuses over the distance of its lateral size L as

$$\tau \approx L^2/D. \tag{10}$$

From Eqs. (7) and (9), the dependence of τ on d is given as

$$\tau \propto d^{(3\nu(3)-2\nu(2)-1)/\nu(3)} = d^{-7/6}. \tag{11}$$

IV. DILUTE SOLUTION IN A THIN SLIT

A. Size of a DNA molecule

The major and minor axes of the binarized fluorescent images of a single DNA molecule are calculated by fitting an ellipsoid to their respective images. The conformation of a DNA molecule fluctuates largely, and the length of its major axis L also varies with time. The distribution of L is shown in Fig. 3. The best-fitted curves in Fig. 3 are the functions suggested by Bonthuis *et al.* [26] for the distribution of the size of a polymer L,

$$P(L) = A \exp\left(-\frac{L^2}{\sigma_1}\right)\exp\left[-\frac{\sigma_2}{(L-L_{\min})^2}\right], \tag{12}$$

where A, σ_1, σ_2, and $L_{\min}$ are the fitting parameters. The formula is for the Gaussian (ideal) chain, but it would be applicable in the first-approximation because the radial distribution itself is close to the multiple of the Gaussian as shown later in Fig. 8 even the SAW is more adequate. $L_{\min}$ is the size of the most tightly packed configuration of the monomers and is expected to be independent of the thickness d. Even though the thickness of the cells used in this study is so thick that the excluded volume interaction in quasi-two dimensions cannot apply, the agreement between experimental results and Eq. (12) is rather good except data for $d=2$ μm.

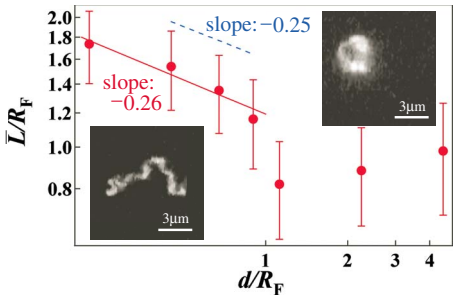

FIG. 4. (Color online) Dependence of the average major length of a DNA molecule $\bar{L}$ on the thickness of a slit d. Both $\bar{L}$ and d are represented in the normalized scale by the Flory radius in three dimensions, $R_F=4.45$ μm. The fluorescent images in a thin (left: $d=1$ μm) and a thick cell (right: $d=10$ μm) are also presented. The exponent of the best-fitted power law drawn as a solid line in the region $d/R_F \leq 1$ is -0.26 ± 0.04. The dotted line shows the power law of $\bar{L} \propto d^{-0.25}$ for a guide to the eyes.

The value of the $L_{\min}$ can be yielded as one of the fitting parameters of Eq. (12) but can be also estimated by another way to judge the fitting validity. The minimum size of the radius of gyration $R_{g\,\min}$ is the half value of R_g [27]. Since the ratio of $R_F/R_g \approx 2.51$ (R_F: the Flory radius in three dimensions) [3] and $R_F = bN^{3/5} = 4.46$ μm (Kuhn length $b=100$ nm and $N=560$) [28], $R_{\min} \sim R_F/2.51/2 = 0.89$ μm. The minimum value of L is estimated to be about 1.78 μm from R_F. The observed values of $L_{\min}$ range from 1.82–2.97 μm. These are larger than the expected values from R_F. This tendency is qualitatively in good agreement with the previous study [26].

In the following discussion, we regard the averaged length of the major axis L over time, $\bar{L}$, as the size of a DNA molecule. The dependence of $\bar{L}$ on the thickness of a slit d is shown in Fig. 4. The values of $\bar{L}$ and d are represented by the normalized scale by the Flory radius in three dimensions, $R_F=4.46$ μm.

In the case of $d/R_F \geq 1$, a polymer is not strongly confined and behaves as one in three-dimensional free space. The observed image at $d=10$ μm is shown as the right picture in Fig. 4. Its overall shape is spherical with high contrast. The length $\bar{L}$ decreases a little bit with decreasing d but is almost same as R_F. Such unusual behavior in the polymer size has been already reported near $d \sim R_F$ by computer simulations [29–31]. The observed decrease of the size is partially due to the attractive interaction by the walls of the slit. Since the effect of the real wall is not simple such as van der Waals and electrostatic interactions, it is difficult to iden-

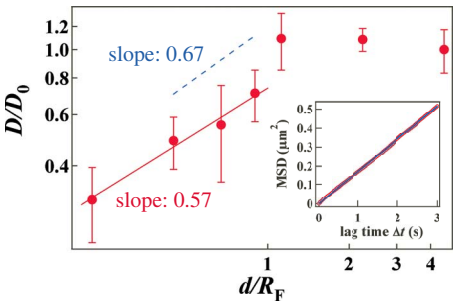

FIG. 5. (Color online) Dependence of the translational self-diffusion coefficient D of a DNA molecule on the thickness of a slit d. Both D and d are represented in the normalized scale by the value of D at $d=20$ μm, $D_0=0.22$ μm^2/s, and the Flory radius in three dimensions $R_F=4.45$ μm. The exponent of the best-fitted power law drawn as a solid line in the region $d/R_F \leq 1$ is 0.57 ± 0.07. The dotted line shows the power law of $D \propto d^{0.67}$ for the guide of eyes. Dependence of MSD on the lag time Δt at $d=1$ μm is plotted in the inset.

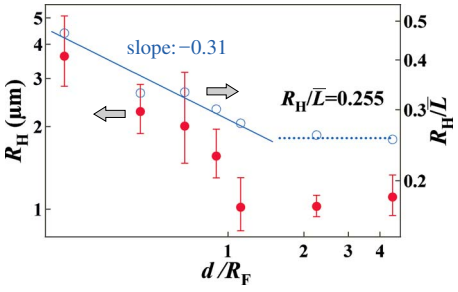

FIG. 6. (Color online) Dependence of the hydrodynamic radius R_H (filled circles: online red) and the ratio of $R_H/\bar{L}$ (empty circles: online blue) of a DNA molecule on the thickness of a slit d. Theoretical ratio of $R_H/\bar{L}=0.255$ in a three-dimensional free space is drawn as a dotted line. The exponent of the best-fitted power law to $R_H/\bar{L}$ in the region of $d/R_F \leq 1$ drawn in a solid line is -0.31 ± 0.05.

tify the reason of the shrinking from the present experimental approach.

In the case of $d/R_F \leq 1$, a polymer is confined to a quasi-two-dimensional space. In this region, the brightness of images decreases, and the shape of a polymer is apparently extended and anisotropic as shown at the left picture in Fig. 4. The distribution of L becomes broader in a thinner cell as shown in Fig. 3. The relatively sharp change of $\bar{L}$ was observed at $d \sim R_F$. The scaling relation $\bar{L} \propto d^{-0.26 \pm 0.04}$ is found within the range of thickness we studied. Although the confinement is not so strong, the dependence of $\bar{L}$ on d approaches that predicted by blob theory $\bar{L} \propto d^{-0.25}$ [Eq. (7)]. This is also consistent with the results reported under much stronger confinement [22,26].

B. Translational self-diffusion of a single DNA

From the temporal change of the center position of the binarized image, MSD can be obtained as is shown in the inset of Fig. 5. MSD is found to be proportional to the lag time Δt. The translation self-diffusion coefficient D can be obtained from the slope of the best-fitted line with Eq. (1). The dependence of D on the thickness of a slit d is shown in Fig. 5. The coefficient D is normalized by that for $d=20$ μm, $D_0=0.22$ μm^2/s. In the case of $d/R_F \geq 1$, D is almost constant. However, D monotonically decreases with decreasing d for $d/R_F \leq 1$. The scaling relation observed in our experiment is $D \propto d^{0.57 \pm 0.07}$. This exponent is smaller than one predicted by blob theory of 0.67 [Eq. (9)]. This discrepancy is probably due to the neglect of hydrodynamic interaction between blobs and that between blobs and walls. Indeed, considering with the results in much narrower slits [23,25], the exponent deviates from this theoretical prediction to the dependence on the thickness of the slit. A more reliable theory with hydrodynamic effect is required to describe the dynamical property of this region. The slight increase in D near $d \sim R_F$ is also due to the unusual decrease of the polymer size discussed in the previous subsection.

The hydrodynamic radius R_H obtained from the dynamic light scattering is often used as the characteristic size of a polymer [3,4]. We can calculate R_H from the translational self-diffusion coefficient D with Stokes-Einstein relation, $D=k_B T/6\pi\eta R_H$, where k_B is the Boltzmann constant, T is the absolute temperature, and η is the viscosity of water (8.9 mPa s at 25 °C). Figure 6 shows the dependence of R_H on d and that of $R_H/\bar{L}$ on d. The value of R_H/R_F is theoretically predicted for a real chain in good solvent as 0.255 [3]. Since the size of a long axis $\bar{L}$ for $d/R_F \geq 1$ is almost same one to R_F, which is shown in the previous subsection, $R_H/\bar{L}$ is expected to be 0.255 for large d. This is confirmed in the region of $d/R_F \geq 1$ as shown in Fig. 6. However, this ratio depends on d as $R_H/\bar{L} \propto d^{-0.31}$ in the region of $d/R_F \leq 1$. This exponent is smaller than that predicted by the blob theory $(-5/12=-0.417)$.

C. Rotational relaxation time of a single DNA

By fitting the binarized images to ellipsoids, the direction of the major axis of a single DNA molecule can be determined. The calculated correlation function of the unit vector parallel to the major axis is shown in the inset of Fig. 7. The correlation function is found to decay exponentially, which is shown as a solid line in the inset. Since the direction of the major axis jumps suddenly due to the change of overall polymer shape, the correlation function cannot be monitored over long time scale. This is the reason why the correlation function does not relax to zero within the lag time we studied. However, the experiments yield enough sequences to discuss this relaxation mode compared to the time scale that was previously reported [26,24]. The calculated rotational relaxation time of a single DNA molecule τ with Eq. (2) is plotted against the thickness of the slit d in Fig. 7. The values of τ are normalized by that at $d=20$ μm, $\tau_0=2.3$ s.

For $d \geq R_F$, τ is almost constant about τ_0. For $d \leq R_F$, τ increases with decreasing d. The scaling relation $\tau \sim d^{-1.07 \pm 0.10}$ is found in our experiment. This exponent is in rather good agreement with the result by Bonthuis *et al.* (-1.17) [26] than that by Hsieh *et al.* (-0.92) [24]. That also

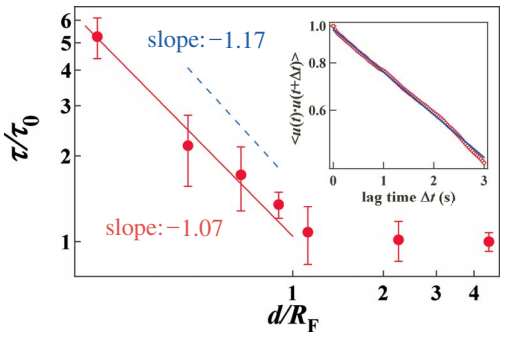

FIG. 7. (Color online) Dependence of the rotational relaxation time τ of a DNA molecule on the thickness of a slit d. Both τ and d are represented in the normalized scale by the experimentally obtained value of τ_0 at $d=20$ μm, $\tau_0=2.3$ s, and the Flory radius in three dimensions $R_F=4.45$ μm. The exponent of the best-fitted power law drawn as a solid line in the region of $d/R_F \leq 1$ is -1.07 ± 0.10. The dotted line shows the power law of $\tau \propto d^{-1.17}$ for the guide of eyes. The time correlation function of the unit vector parallel to the major axis at $d=1$ μm is plotted in the inset as a semilogarithmic plot.

makes good agreement with the predicted exponent by blob theory −1.17. The experimentally obtained exponent −1.07 is also consistent with the exponent calculated from Eq. (10), −1.09, using the experimentally obtained relations $\bar{L} \sim d^{-0.26}$ and $D \sim d^{0.57}$.

D. Radial distribution function of segments in a single DNA

The analysis in the previous subsections is based on the binarized fluorescent images of a single DNA molecule, but the intensity of fluorescent image reflects the density of segments [32]. In this subsection, the grayscale images of a single molecule have been used to calculate the radial distribution function of segments in a molecule around its center of mass. The distribution function $n(r)/n_{\max}$ was calculated as the total intensity at a certain radius r normalized by its maximum value $n_{\max}$. The value $n(r)$ relates the usually used radial distribution function $g(r)$ as $n(r)=2\pi r g(r)$. The radial distribution functions of segments $n(r)/n_{\max}$ at various thicknesses are shown in Fig. 8. $n_{\max}$ is the maximum number of segments in the distribution function and the corresponding distance is denoted by $r_{\max}$. The distance $r_{\max}$ and the width of the distribution monotonically increases with decreasing the thickness. The dotted curve in Fig. 8 is the radial distribution of segments in the two-dimensional Gaussian chain with the same Kuhn length and the same number of segments.

We have compared the obtained experimental results with the distribution of segments in an excluded volume chain calculated from the coordinate data of segments obtained by Monte Carlo simulation [33,34]. From the simulated three-dimensional coordinate data of the segments, the distribution of the segments projected onto the two-dimensional plane that contains the center of mass of a polymer was calculated and is shown as a thick solid line in Fig. 8. The segment distribution in an excluded volume chain shows better agreement with the experimental ones compared to a Gaussian

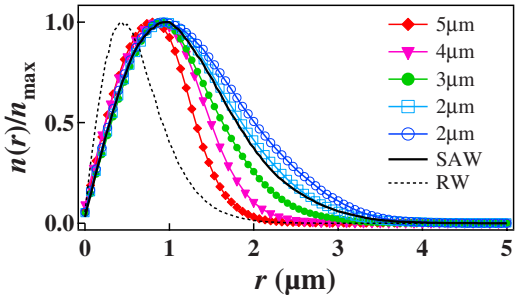

FIG. 8. (Color online) Radial distribution function of segments around the center of mass of a single DNA molecule in a slit with different thickness. The thick solid curve is calculated from the coordinate data of segments in the two-dimensional projection of the excluded volume chains in three-dimension obtained by computer simulation. The dotted curve is the distribution function of the segments in the two-dimensional Gaussian chain.

chain. However, it is apparently different from the experimentally obtained one for large d.

One of the reasons for this discrepancy is the existence of the segments out of the focal plane of a microscope. When d is large, the considerable number of segments is out of focal plane, and the distribution differs from one expected for an ideal excluded volume chain. This is one reason why we utilized the binarized images in the previous subsections. In the case of small d, since almost all the segments can be

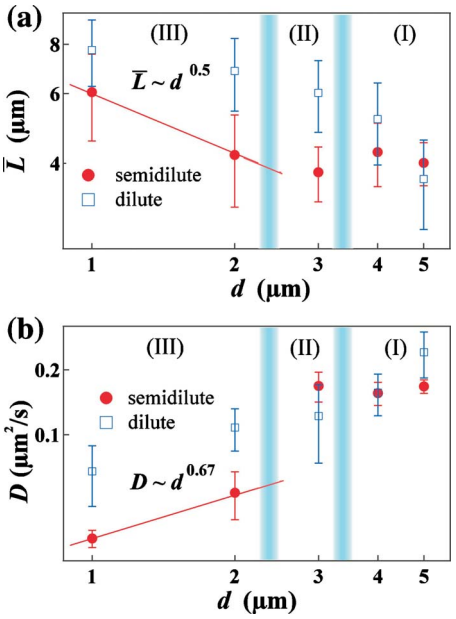

FIG. 9. (Color online) Dependence of (a) the length of the major axis $\bar{L}$ and (b) the translational self-diffusion coefficient D of a single DNA molecule on the thickness of a slit d. The open squares (online blue): dilute solutions. The filled circles (online red): semidilute solutions. The solid line in (a) indicates $\bar{L} \propto d^{-1/2}$ and that in (b) indicates $D \propto d^{2/3}$ for the guide of eyes. The regions marked by (I), (II) and (III) are calculated from the phase diagram [20,35].

detected, the obtained distribution approaches ideal one. Actually, we have calculated the radial distribution function of the simulated excluded volume chain sliced with a finite thickness to confirm our assumption. As the width of the sliced region increases, the peak position r_{max} decreases. Therefore, r_{max} in thicker cells will shift to smaller value than that expected in an exclude volume chain. This behavior qualitatively agrees with our experimental observation in Fig. 8. The size estimated from the grayscale images becomes smaller because the weight of the parts near the center increases. On the other hand, the size estimated from binarized images relatively enlarges because the weight of the outer side increases. Since almost all the segments can be detected in the previous reports for much thinner slits, the grayscale images offer much accurate estimation of the polymer size. However, from the comparison to computer simulation, the analysis based on binarized images offer more reliable results in thick samples used in the present study.

V. SEMIDILUTE SOLUTION IN A THIN SLIT

In dilute solutions, the influence of spatial confinement clearly becomes serious in the region where the slit size d is smaller than the size of a polymer R_F. This is experimentally confirmed in the previous section. The upper boundary of the dilute regime is the overlap concentration c^* where the spheres of radius R_F start to overlap. This is 21.1 μM for T4GT7 DNA used in this study. Above c^*, polymers are in the so-called semidilute regime. In semidilute solutions, polymers overlap, and entangle each other in more concentrated solutions. This topological confinement by other polymers drastically changes the dynamical properties of polymers in semidilute solutions.

The influence of confinement by a slit is expected to be small in semidilute solutions because the interaction between polymers is screened within the length of the blob size that corresponds to the mesh-size of the entangled polymer networks. As the blob size becomes smaller by increasing polymer concentration, the critical thickness where the influence of slits is serious becomes smaller. In this section, we study the influence of a slit in a semidilute solution. The static structure of a polymer in a slit has been studied by the scaling theory. The phase diagram of a polymer confined in a slit was studied in concentration-thickness space [20,35]. In semidilute region, there are three regions: (I) semidilute sphere, (II) three-dimensional semidilute confined sphere, and (III) two-dimensional semidilute pancake. The influence of confinement by slits increases in this order. In the regions (I) and (II), the influence of concentration is much stronger than that of spatial confinement. On the contrary, the influence of spatial confinement is more serious than that of concentration in the region (III).

In this section, the influence of confinement by slits on the size and the translational self-diffusion of a polymer were studied in a semidilute solution. From the phase diagram, the effect of confinement in a rather thick cell is more significant near c^*. The concentration of a DNA solution was fixed to $c=1.56c^*$ as an example.

Figure 9(a) shows the dependence of the length of the major axis $\bar{L}$ on the thickness of a slit d. The result for a dilute solution is also plotted in Fig. 9(a). The influence of the concentration to the size of a polymer is rather small in semidilute solutions. The size $\bar{L}$ in the thick slits is almost same both in dilute and semidilute solutions (see the data at $d=5$ μm). The boundary thicknesses between the different regions calculated from the phase diagram are respectively drawn as blurred lines. The size in the region (I) and (II) are almost same as the Flory radius in three dimensions. However, $\bar{L}$ in the region (III) significantly increases with decreasing d. This indicates that the influence of confinement is weaker than that in dilute solutions. From the scaling theory, $\bar{L}$ is scaled as $\bar{L} \propto d^{-1/2}$ in semidilute solutions [20]. This is in good agreement with the obtained dependence of $\bar{L}$ in Fig. 9(a) in the region (III).

Figure 9(b) shows the dependence of the translational self-diffusion coefficient D on the thickness of a slit d. The result for a dilute solution is also plotted in Fig. 9(b). The obtained D at $d=5$ μm in a semidilute solution is smaller than that in dilute one. This is mainly due to the overlapping effect of polymers. The difference of D between in the regions (I) and (II) is not significant as is the same as in $\bar{L}$. However, it suddenly decreases in the region (III) and strongly decreases with decreasing d in this region. The dependence of D on d in the region (III) seems to be scaled with the same exponent in a dilute solutions as $D \propto d^{2/3}$.

From our limited results, the confinement effect becomes serious only at the region (III) in a semidilute solution. This is the transition from three-dimensional to two-dimensional confinement and corresponds to one observed at $d \sim R_F$ in dilute solutions. In a qualitative speculation, it is reasonable the dynamical property, i.e., diffusion, changes around the condition where the polymer size $\bar{L}$ changes. The condition $d>R$ permits free diffusion, but the region $d<R$ limits free diffusion and only permits overlapping motion. The reptation motion or excluded motion will be observed in more concentrated solutions. The width of the region (II) is too narrow to study its physical properties in this study. It is necessary to study more concentrated solutions to draw a quantitative conclusion on the difference of the physical properties in respective regions. The more precise experiment in a wider range of concentrations in semidilute solutions is under performed.

VI. CONCLUSION

We studied the conformation and dynamics of a single DNA molecule in a thin slit using a fluorescent microscope. In a dilute solution, the dependence of its conformation and dynamics on the thickness of a slit shows relatively sharp change at the same thickness as the Flory radius of a DNA in three dimensions. The blob picture is relatively in good agreement with the obtained average polymer size, translational self-diffusion coefficient, and rotational relaxation time in thinner cells. Besides these overall properties of a polymer, the radial distribution of segments has been

calculated from the grey scaled images of a single DNA molecule. We find the finite focal depth makes serious influence on the measurement of the distribution of segments. The influence of confinement on the size and diffusivity of a polymer have been also studied in a semidilute solution near the overlap concentration. Its effect is slight in comparison with that in a dilute solution in three-dimensional regions. However, the serious influence is also apparent in the region called two-dimensional semidilute pancakes in the phase diagram.

ACKNOWLEDGMENTS

This work is financially supported by a Grant-in-Aid for Scientific Research from JSPS and by Priority Area "Soft Matter Physics" from MEXT, Japan. The authors thank Mr. K. Shimomura, Professor H. Nakanishi and Professor N. Mitarai (now at the Niels Bohr Institute) at Kyushu University for their comments and providing the simulation data on excluded volume chains.

[1] P. G. de Gennes, *Scaling Concepts in Polymer Physics* (Cornell University Press, Ithaca, 1972).
[2] M. Doi, *Introduction to in Polymer Physics* (Oxford University Press, Claredon, 1996).
[3] I. Teraoka, *Polymer Solutions* (Wiley Inter-Science, New York, 2002).
[4] In the case of DNA, for examples, S. S. Sorlie and R. Pecora, Macromolecules **21**, 1437 (1988); R. Borsali, H. Nguyen, and R. Pecora, *ibid.* **31**, 1548 (1998).
[5] C. Frontali, E. Dore, A. Ferrauto, E. Gratton, A. Bettini, M. R. Pozzan, and E. Valdevit, Biopolymers **18**, 1353 (1979).
[6] H. G. Hansma, K. J. Kima, D. E. Laneya, R. A. Garciab, M. Argamanc, M. J. Allend, and S. M. Parsonse, J. Struct. Biol. **119**, 99 (1997).
[7] G. Witz, K. Rechendorff, J. Adamcik, and G. Dietler, Phys. Rev. Lett. **101**, 148103 (2008).
[8] S. Matsumoto, K. Morikawa, and M. Yanagida, J. Mol. Biol. **152**, 501 (1981).
[9] M. Matsumoto, T. Sakaguchi, M. Kimura, M. Doi, K. Mingawa, Y. Matsuzawa, and K. Yoshikawa, J. Polym. Sci., Part B: Polym. Phys. **30**, 779 (1992).
[10] D. E. Smith, T. T. Perkins, and S. Chu, Macromolecules **29**, 1372 (1996).
[11] C. Haber, S. A. Ruiz, and D. Wirtz, Proc. Natl. Acad. Sci. U.S.A. **97**, 10792 (2000).
[12] T. T. Perkins, D. E. Smith, and S. Chu, Science **264**, 819 (1994).
[13] Y. Masubuchi, H. Oana, K. Ono, M. Matsumoto, M. Doi, K. Minamigawa, Y. Matsuzawa, and K. Yoshikawa, Macromolecules **26**, 5269 (1993).
[14] T. T. Perkins, S. R. Quake, D. E. Smith, and S. Chu, Science **264**, 822 (1994).
[15] R. G. Larson, T. T. Perkins, D. E. Smith, and S. Chu, Phys. Rev. E **55**, 1794 (1997).
[16] S. R. Quake, H. Babcook, and S. Chu, Nature (London) **388**, 151 (1997).
[17] M. Ichikawa, Y. Matsuzawa, and K. Yoshikawa, J. Phys. Soc. Jpn. **74**, 1958 (2005).
[18] M. Ichikawa, H. Ichikawa, K. Yoshikawa, and Y. Kimura, Phys. Rev. Lett. **99**, 148104 (2007).
[19] P. Pincus, Macromolecules **9**, 386 (1976).
[20] M. Daoud and P. G. de Gennes, J. Phys. **38**, 85 (1977).
[21] B. Maier and J. O. Rädler, Phys. Rev. Lett. **82**, 1911 (1999).
[22] Y.-L. Chen, M. D. Graham, J. J. de Pablo, G. C. Randall, M. Gupta, and P. S. Doyle, Phys. Rev. E **70** 060901(R) (2004).
[23] A. Balducci, P. Mao, J. Han, and P. S. Doyle, Macromolecules **39**, 6273 (2006).
[24] C.-C. Hsieh, A. Balducci, and P. S. Doyle, Macromolecules **40**, 5196 (2007).
[25] A. Balducci, C.-C. Hsieh, and P. S. Doyle, Phys. Rev. Lett. **99**, 238102 (2007).
[26] D. J. Bonthuis, C. Meyer, D. Stein, and C. Dekker, Phys. Rev. Lett. **101**, 108303 (2008).
[27] D. I. Dimitrov, A. Milchev, K. Binder, L. I. Klushin, and A. M. Skovortsov, J. Chem. Phys. **128**, 234902 (2008).
[28] P. J. Hagerman, Annu. Rev. Biophys. Biophys. Chem. **17**, 265 (1988).
[29] J. H. van Vliet and G. ten Brinke, J. Chem. Phys. **93**, 1436 (1990).
[30] J. H. van Vliet, M. C. Luyten, and G. ten Brinke, Macromolecules **25**, 3802 (1992).
[31] E. A. Strychalski, S. L. Levy, and H. G. Craighead, Macromolecules **41**, 7716 (2008).
[32] N. Yoshinaga and K. Yoshikawa, J. Chem. Phys. **116**, 9926 (2002).
[33] The coordinate values of the excluded volume chains in three dimensions calculated by Monte Carlo simulation with bond fluctuation model on a lattice have been kindly provided by Mr. K. Shimomura at Kyushu University. The number of segments was set to 512. The total number of the generated polymers is 1000. The detail of the simulation method is found in [34].
[34] K. Shimomura, H. Nakanishi, and N. Mitarai,Phys. Rev. E **80**, 051804 (2009).
[35] Y. Wang and I. Teraoka, Macromolecules **33**, 3478 (2000).